



Improved Well Drilling Simulation With Transient Thermal Model For Predicting Wellbore Temperatures

Mostafa M. Abdelhafiz^{1,2}, Joachim F. Oppelt¹, Luiz A. Hegele Jr. ³

¹*Drilling Simulator Celle, Clausthal University of Technology
Zum Drilling Simulator-1, 29221, Celle, Germany
mostafa.abdelhafiz@tu-clausthal.de
joachim.oppelt@tu-clausthal.de*

²*Faculty of Engineering and Technology, Future University in Egypt
End of 90th St., Fifth Settlement, 11835, Cairo, Egypt*

³*Department of Petroleum Engineering, Santa Catarina State University
88336-275, Balneário Camboriú, Brazil
luiz.hegele@udesc.br*

Abstract. Drilling simulators have been utilized as a key for drilling optimization and cost reduction for the drilling process. Supporting the drilling simulator with realistic and accurate models can enhance the simulation processes leading to a more efficient drilling operation. This paper presents the implementation of a newly developed temperature model in the software simulator at Drilling Simulator Celle (DSC). The model can simulate and predict the temperature of the wellbore fluids, drill string, casing, cement, and the surrounding formation for depth and time. The model is also able to simulate both the flowing condition of the drilling fluids and the static condition or the so-called thermal recovery period. The model is embedded into the drilling simulator through an application-programming interface (API) which allows the communication between each model and the drilling simulator itself. The user of the simulator can monitor the wellbore system temperature at each depth in real-time or even in accelerated mode. This allows the pre-drilling of the well on the simulator in the design and planning phase. For application and demonstration purposes, a case study has been conducted for a geothermal well in the Hanover (Germany) area. The historic data has information about the formation, drill string, and bottom hole assembly, as well as operational parameters. Different simulation runs have been conducted using the drilling simulator, and the transient behaviour of the wellbore temperature is analyzed during circulation and shut-in periods.

Keywords: Thermal Modeling, Simulation, Drilling, Circulation.

1 Introduction

The heat transfer process between the wellbore fluids and the surrounding formation, casing, and cement can affect all phases of the well design. These include the design of the drilling fluid, cement slurry, and the electronic components used in the measurement during the drilling[1–4]. The drilling fluid temperature has a significant effect on the fluid rheological properties. Different research efforts have been conducted aiming to model the effect of the temperatures on the drilling fluids properties[5–8]. They have concluded that the temperature is heavily affecting the drilling fluid viscosity, yield point, gel strength, and density. These properties can significantly affect the drilling process; inadequate viscosity of the drilling fluid may lead to extensive wellbore cleaning problems. Viscosity is also affecting the annular pressure losses, which affect the value of the ECD[9]. This value is critical and especially during drilling wells with narrow mud windows, which is the margin between the pore pressure and the fracture pressure.

Moreover, Zhang et al. [3] presented the influence of temperature on wellbore stability, especially for geothermal drilling applications. They have concluded that significant damage of the borehole walls can be resulted from the temperature recovery during drilling geothermal wells. This results from the effect of the temperature variation on the mechanical properties of the rock. They have also shown the effect of the thermal recovery periods where

the circulation stops on the wellbore stability.

Another researches such as Choi and Tan [10], Chen and Ewy [11], and AlBahrani et al. [12] have considered the time-dependent wellbore stability issues resulting from the drilling fluid temperature variations. In their work, they have shown the temperature difference between the circulating fluid and the surrounding formation rock can result in a contraction of the rock grains in the wellbore wall, which may cause a reduction in the hoop stresses. This depends on the formation rock thermal expansion coefficient and the porosity. Another important aspect regarding the thermal effects on the wellbore stability arises during drilling in gas hydrates reservoirs. Li et al. [13] explored the temperature effect on the disintegration of the wellbore walls of the gas hydrates reservoirs. They have obtained a relationship between the drilling fluid temperature and the borehole enlargement.

Furthermore, the temperature of the wellbore can affect many parameters during cement slurry design. Numerous researches have noted the direct effect of the temperature on the thickening time, compressive strength, and the rheology of the cement during pumping. The temperature has a direct impact on the primary chemical reactions that control the hydration of the cement slurry. Overestimating or underestimating the wellbore temperature will result in a variety of non-productive time events, ranging from excessive Wait On cement (WOC) to drilling out of cementing of the casing [14].

This results in the importance of accurate modelling and simulation of the borehole temperature and the surrounding formation during drilling. Accurate estimation and simulation of those temperatures should be supported by a comprehensive dynamic study of the heat transfer between the wellbore fluid and the surrounding formation.

2 Governing Equations

The set of thermal balance equations that describes the thermal behaviour of the borehole and the surrounding environment is acquired from our previous work Abdelhafiz et al. [15]. This set of equations divides the wellbore system into two main zones. The first zone is the "wellbore zone", which contains the fluid inside the drill pipe with a temperature of $T^{(P)}$, the solid walls of the drill pipe with a temperature of $T^{(S)}$, and the fluid in the annulus with a temperature of $T^{(A)}$. The second section is the "post wellbore zone" with a temperature of $T^{(PW)}$. This zone includes the casing strings, the cement behind the casing, and the formation rock.

The thermal balance equation for each section is as follows [15]:

$$\frac{\partial (\rho_P c_{p,P} T^{(P)})}{\partial t} + \frac{\partial (\rho_P c_{p,P} T^{(P)} u_P)}{\partial z} = -\frac{2h_P}{r_{P,in}} (T^{(P)} - T^{(S)}) + \frac{\partial}{\partial z} \left(k_P \frac{\partial T^{(P)}}{\partial z} \right), \quad (1)$$

$$\frac{\partial (\rho_S c_{p,S} T^{(S)})}{\partial t} = -\frac{2h_P r_{P,in}}{r_{P,out}^2 - r_{P,in}^2} (T^{(S)} - T^{(P)}) - \frac{2h_{A,in} r_{P,out}}{r_{P,out}^2 - r_{P,in}^2} (T^{(S)} - T^{(A)}) + \frac{\partial}{\partial z} \left(k_S \frac{\partial T^{(S)}}{\partial z} \right), \quad (2)$$

$$\begin{aligned} \frac{\partial (\rho_A c_{p,A} T^{(A)})}{\partial t} + \frac{\partial (\rho_A c_{p,A} T^{(A)} u_A)}{\partial z} = & -\frac{2h_{A,in} r_{P,out}}{r_A^2 - r_{P,out}^2} (T^{(A)} - T^{(S)}) \\ & - \frac{2h_{A,out} r_A}{r_A^2 - r_{P,out}^2} (T^{(A)} - T^{(PW)}) + \frac{\partial}{\partial z} \left(k_A \frac{\partial T^{(A)}}{\partial z} \right), \end{aligned} \quad (3)$$

$$\frac{\partial (\rho_{PW} c_{p,PW} T^{(PW)})}{\partial t} = \frac{\partial}{\partial z} \left(k \frac{\partial T^{(PW)}}{\partial z} \right) + \frac{1}{r} \frac{\partial}{\partial r} \left(rk \frac{\partial T^{(PW)}}{\partial r} \right), \quad (4)$$

where the superscript A, P, S and PW denotes annulus, pipe, pipe wall and post wellbore sections respectively. ρ , c_p and k along with the subscript (P, S and A) are the density, the specific heat capacity and the conductivity index of the pipe fluid, pipe wall and the annulus fluid respectively. The symbols h_P , $h_{A,in}$ and $h_{A,out}$ are the convective heat transfer coefficients for the pipe and the inner and outer annulus walls respectively. The radii $r_{P,in}$, $r_{P,out}$, and r_A represent the drill pipe inner, outer and the annulus radius respectively. Finally, u_P and u_A are the fluid velocity inside the pipe and the annulus. As can be seen from Eq.(1 to 3), the radial heat transfer between the wellbore fluids and the surroundings is considered using the local convective heat transfer coefficients (h) [16]. By that, the thermal energy balance equations are decoupled from the momentum equation. In other words, the heat transfer in the radial direction is only a function of the convective heat transfer coefficient, not the velocity profile or the pressure gradient. This approach is valid in the fully developed flow, as the local convection coefficient becomes constant [17].

Additional heat is generated at the interface between the drill bit and the rock formation due to friction, which is derived from the relative rotating motion between the bit cutters and the formation. The amount of heat generated is related to the drill bit cutting mechanism. Shear cutting drill bits like polycrystalline diamond compact (PDC)

bits have been widely used in the drilling industry for oil and gas wells and geothermal wells[18]. The cutting mechanism of that type of drill bit leads to generate a considerable amount of heat due to friction.

According to Glowka and Stone [19], the total heat rate generated due to friction per unit area is:

$$Q_{friction} = \frac{f F_N v}{A_c}, \quad (5)$$

where $Q_{friction}$ is the heat rate generated due to friction (W/m^2), f is the coefficient of dynamic friction between the bit cutters and the formation. F_N is the normal force acting in the drill bit which can be considered as the weight on bit. (N), v is the cutting speed (m/s) which is derived from the bit rotational speed ω multiply the hole radius (r_a). Finally, A_c is the contact surface area between the drill bit and the formation (m^2). This additional heat generation should act as a heat source at the bottom of the well which is added to the bottom boundary condition which considers the frictional heating and convective cooling.

For the shut-in condition, a thermal balance for heat transfer by conduction tool place as following:

$$\dot{E}_{str} = \Delta \dot{E} \Big|_{(rdl)} + \Delta \dot{E} \Big|_{(axl)}, \quad (6)$$

where \dot{E}_{str} is the energy stored, (rdl) and (axl) denotes for the radial and the axial directions respectively. $\Delta \dot{E} = \dot{E}_{in} - \dot{E}_{out}$. This equation is then applied for each section of the wellbore zones and discretized as explained in the following section.

The equations have been discretized by the means of the finite volume method(FVM). The first-order upwind scheme is utilized for the advective term. The fully explicit linear approximation is used for the time integration[15, 16].

3 DrillSim-600

The Drill-Sim 600 is an advanced virtual drilling simulator provided by the company Drilling Systems[20]. The simulator is mainly offering drillers and operators to train on the drilling and the well control operation. Along with the graphical representation, the simulator combines several mathematical models to describe the physical phenomena at the surface and the downhole during the drilling process.

The simulator has four main components as shown in Fig. 1 The first is the student station (Fig. 1a). Here, the user has control over all the drilling rig systems such as mud pumps, draw works and top drive, and also the well control unit. In front of the chair, additional screens that show the current drilling parameters for real-time monitoring as the weight on bit, rpm, torque, rate of penetration (ROP), hook load, mud flow rate in and out, and pump pressure. At the front, eight large screens display the view of the actual driller position to mimic the real situation.

The second part is the instructor station (Fig. 1b). This is considered the control interface to the simulator where sitting up the simulation scenario took place. Monitoring the downhole parameter is also possible from the instructor station. From there, one can monitor the well control status and the wellbore integrity. Additionally, the instructor can also add an artificial malfunction to one of the drilling rig components for training purposes.

Besides the instructor station, the API work station is located. Here, All the external downhole models are implemented. More details about the API workstation are in the next section.

The last part act as the brain of the simulator is the computing and graphical processing unit. This unit is responsible for processing all the needed calculations from the downhole physical model to simulate the drilling process. It also processes all the graphical output in real-time.

3.1 Drill-Sim 600 application programming interface (API)

The API is generally considered as a communication software that connects between different computers or between different computer programs.

Figure 2 illustrates the communication through the API with the simulator and the external models implemented on the API workstation. The API acts as a door where the inputs needed for the implemented model can be obtained. And also the final output values from the model can be sent back to the simulator. As an example for the thermal model, The mathematical equations and the solution algorithm is written in a computer code with C# as a programming language. The code is implemented on the API workstation. The algorithm calls for initial wellbore construction data like borehole diameter, drill string design, drilling fluid properties, and initial depth. Additional

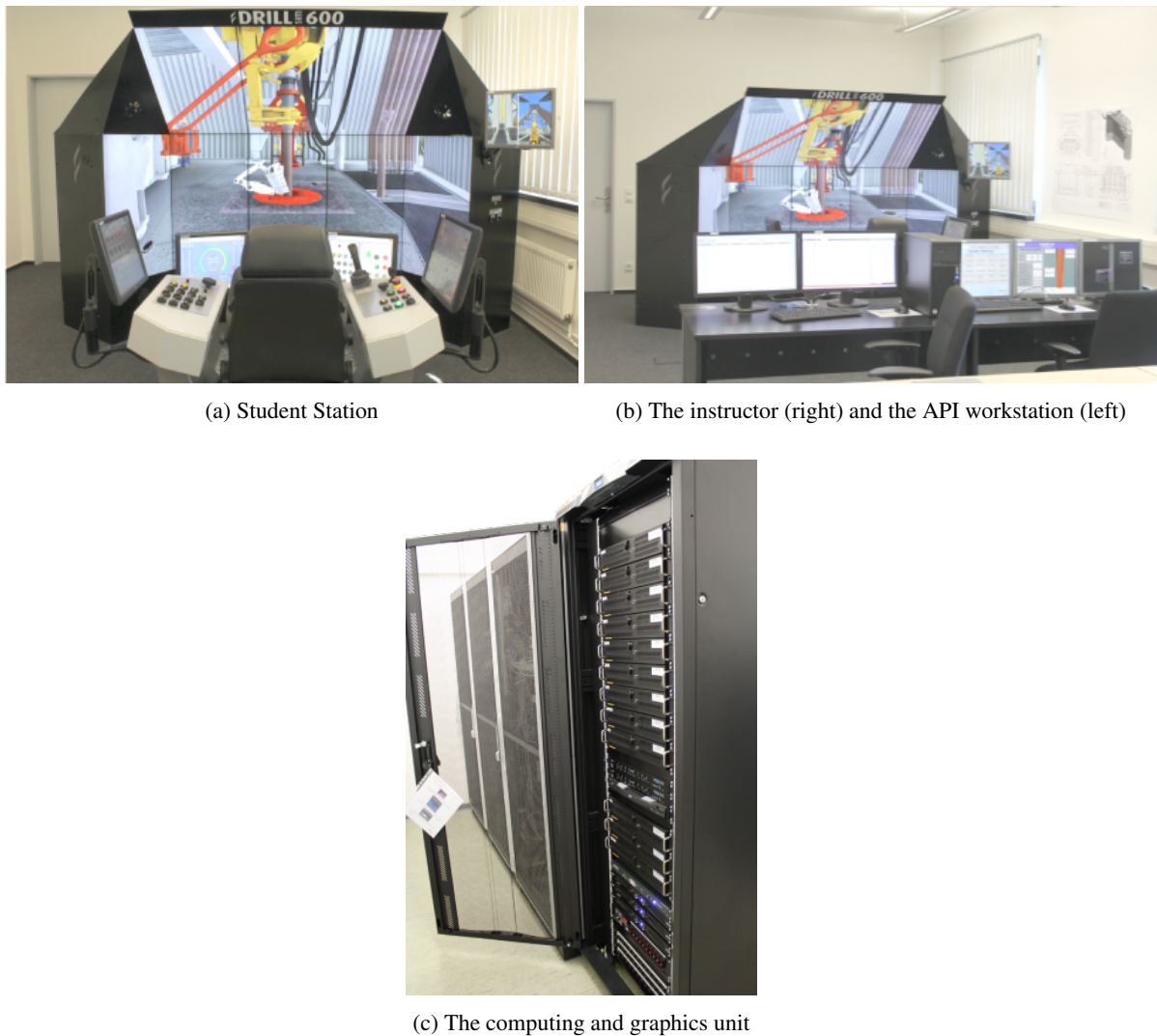


Figure 1. Main components of the Drilling simulator Drill-Sim 600

important parameters that are not available from the simulator as the thermal properties of the formation, drill string, and drilling fluid are set directly from the API work station via a graphical user interface as going to be discussed later. Other variables are changing with time such as flow rate, current depth, bit RPM.

The model then runs on the API workstation calculating the temperature of the wellbore system at that time step according to the operational parameters acquired from the simulator. Ideally, The temperature is set back to the simulator at the current step. However, currently, the simulator does not have a temperature module. Therefore the calculated temperature remains at the API workstation for real-time visualization.

Cooperation with the simulator provider company is taken place therefore a temperature module is created to set and update the temperature with time. This will be an input for the temperature-dependent properties model as viscosity with lead to more realistic simulations.

One important feature of such a communication interface is the abstraction. The API hides all the internal details of the system that the communication is done with, and only exposes the parts or variables that are needed for the communication[21]. This can lead to more robust and more flexible to future changes in the main code. Another important advantage in the case of Drill-Sim 600 is that the commercial company can keep all their code parts closed and confidential and also provide a way for scientific development.

3.2 Solution Algorithm

The discretized set of equations described in section 2 are coded using visual C# Windows Forms. Figure. 3 shows the main blocks in the code. The program starts with loading the static input parameters into the memory.

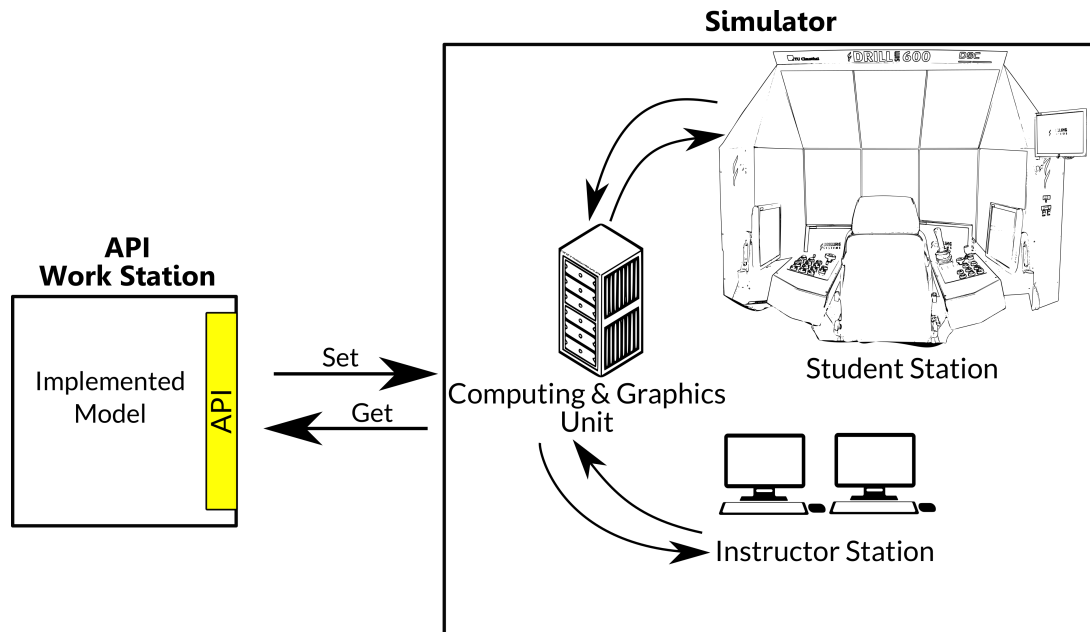


Figure 2. Sketch illustrating the communication between the Drilling simulator with external implemented models through the API

The available input parameters from the simulator Drill-Sim 600 are called via the API. The other parameters are then called from the input window is will be discussed in section 3.3. The second block is to initialize the simulation state where the initial conditions are set. The third block is where the actual simulation takes place. Here the thermal balance equations are solved for each grid volume each time step. The simulation block, continues updates in the dynamic variables are considered. In addition to updating the results in the graphical window in real-time. A more detailed description of the third block algorithm is shown in fig. 4.

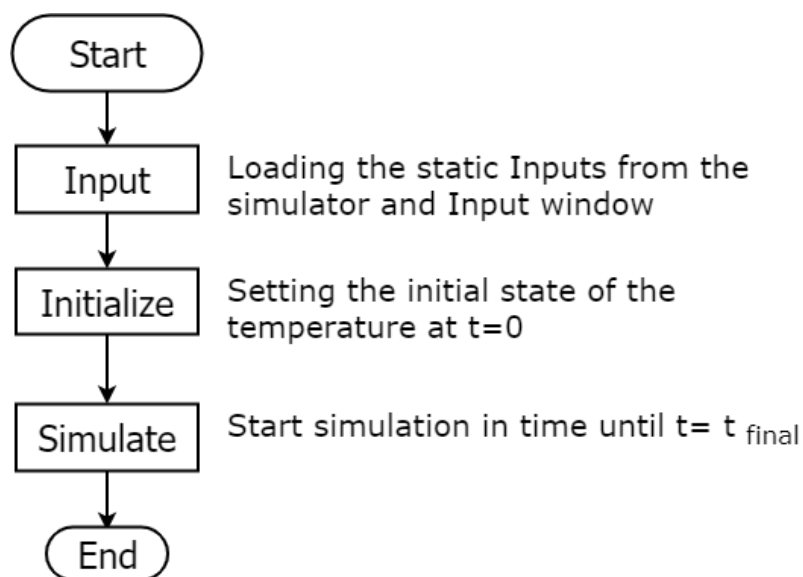


Figure 3. Flow chart for the basic blocks of the solution algorithm

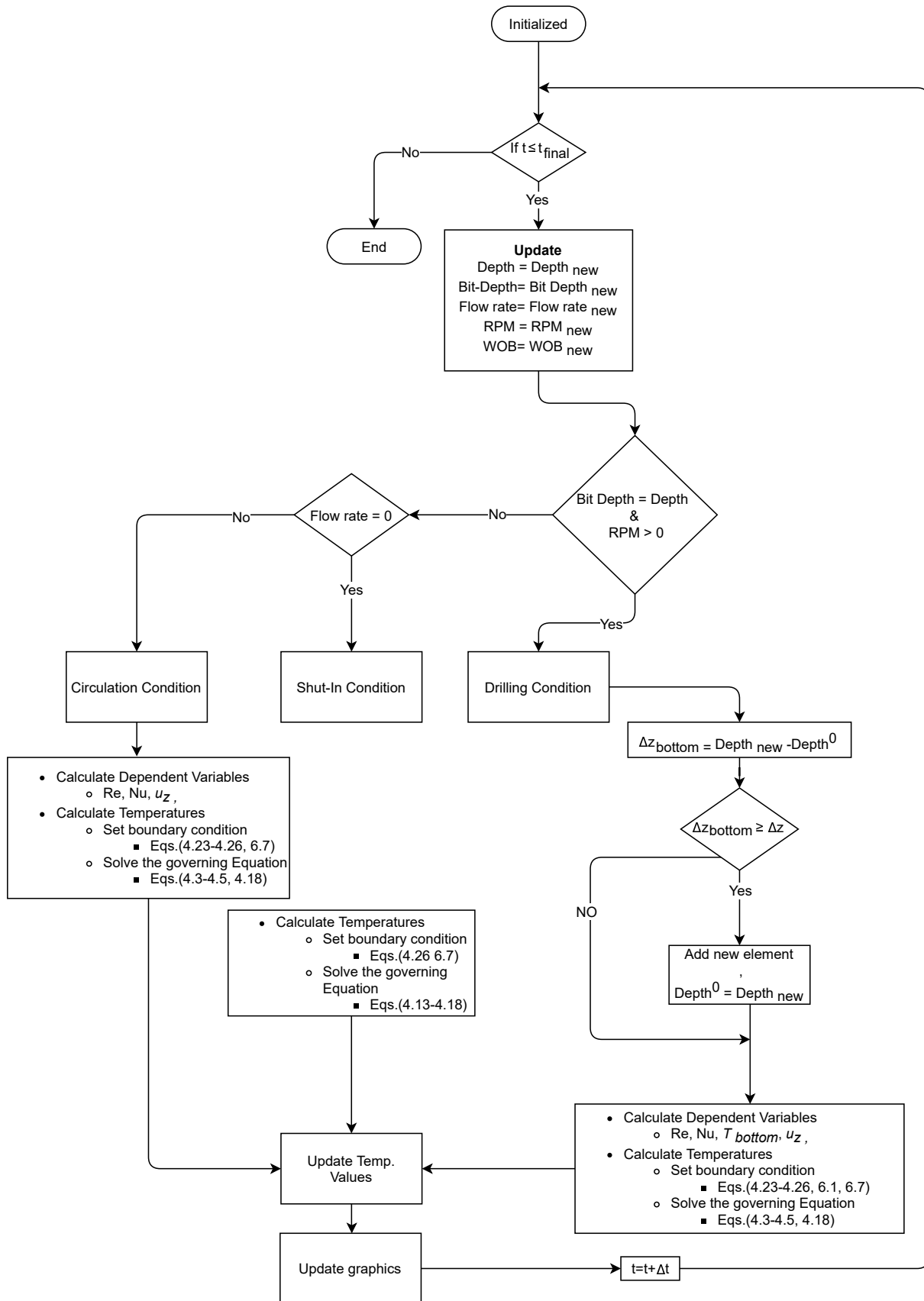
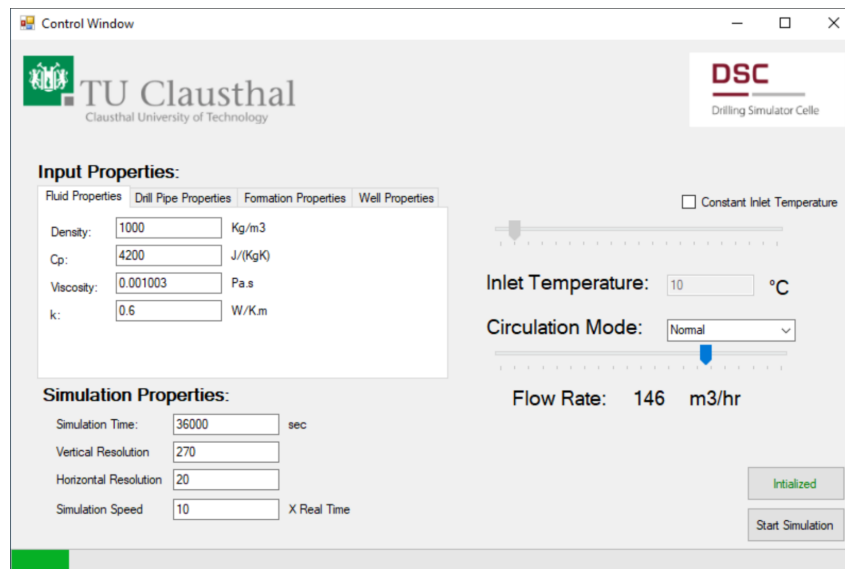


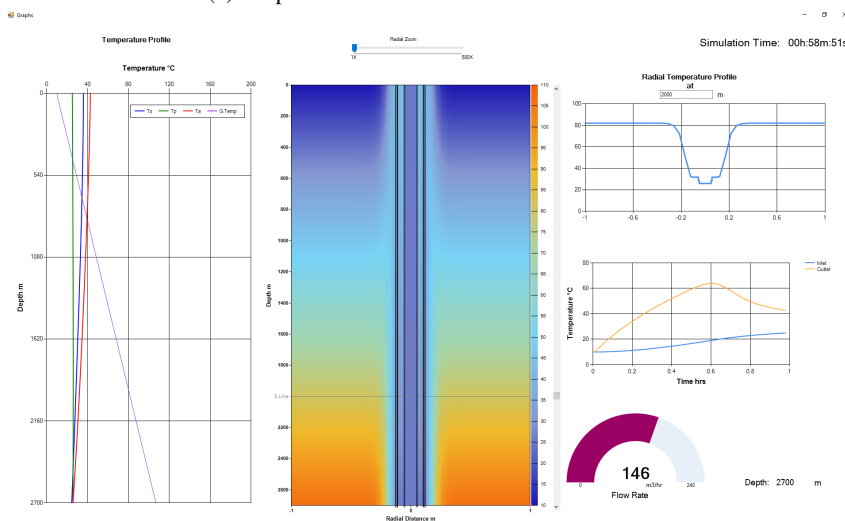
Figure 4. Detailed flow diagram for the solution procedure of the transient simulation block

3.3 GUI

To facilitate the use of the model for more efficient simulation runs, a graphical user interface (GUI) has been developed. The GUI aid the user to adjust the input parameters to the model without going through the code itself which makes it more user-friendly. As discussed earlier, the input for the thermal model comes from two sources which are the Drill-Sim 600 and additional inputs by the user. To make the code functional even on its own, all the input parameters can be controlled through the GUI. In case the API is available, the input variables are taken from the Drill-Sim 600. Figures 5a and 5b shows a snapshots from the control wand the results windows of the GUI.



(a) Snap shot of the control window of the GUI



(b) Snap shot of the graphical results window of the GUI

Figure 5. Graphical User Interface

4 Application and results

In this section, an actual geothermal well is selected for the application of the developed model. The selected well is a part of the GeneSys project, which aims to extract the geothermal heat energy from low permeability sedimentary rocks with a single well concept. The geothermal well Groß Buchholz Gt1 (GB-GT1) is located in the Hannover area, Northern Germany.

The stratigraphic column, and the actual wellbore plan as well as casing setting depths and sizes of the GB-GT1 well can be seen in Fig.6. The well has a total depth of 3901 m targeting the lower Buntsandstein formation. A conductor casing of size 601 mm is set at depth 38.5 m followed by drilling the surface hole section with a drill bit size of 17½ in to depth 1175 m. The surface casing is set in the Wealden formation with a size of 13⅜ in. The intermediate hole with size of 12¼ in is drilled to a depth of 2876 m and the intermediate casing was set with a size 9⅝ in. Finally, the production hole with size 8½ in is drilled reaching the target depth at 3901 m with a maximum deviation angle of 30°.

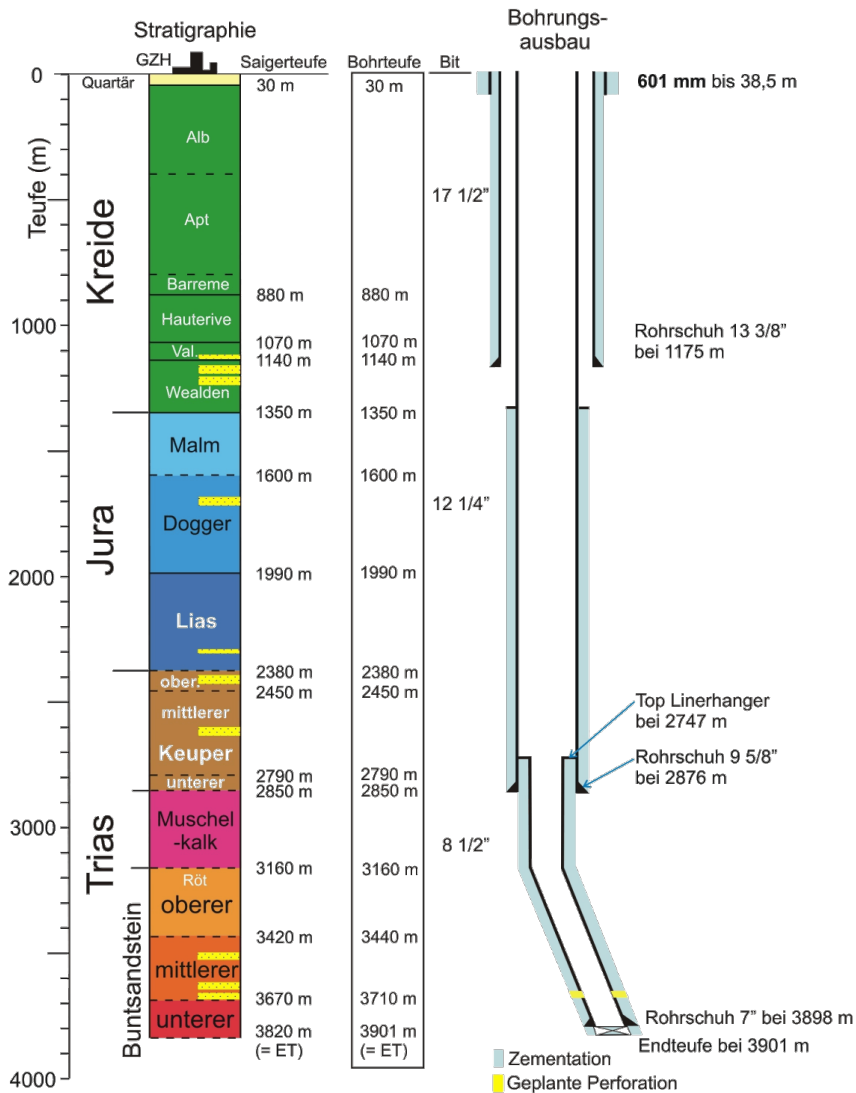


Figure 6. Stratigraphic column and wellbore sketch of well completion of geothermal well GB-Gt1[22]

The first step for conducting this simulation is to select the time interval to be simulated. The optimum time interval for conducting the thermal simulation and comparison with the measured data from the GBGT-1 well is the 20 hours interval between the depths 1250.5 m and 1368 m as it is preceded by a long shut-in duration, and an initial temperature equivalent to the geothermal gradient can be assumed.

The simulation is performed for the described section using 500 cells in the vertical direction, and 30 cells in the radial direction. Figure 7 represents screen capture of the final temperature state resulted from the temperature simulation of the GBGT-1 well. The window consists of five different subplots. On the top, a contour plot represents the wellbore system temperature. The x-axis represents the depth, the y-axis represents the radial distance from the borehole centre and the colour represents the temperature. On the figure, different components which have been included in the simulation are outlined. In the middle, the drill string with different cross-sections is clearly shown. The conductor and the surface casings are also outlined. The mud tank temperature is represented with the same colour map of the wellbore system temperature. For the bottom part of the figure, on the left side of the figure, the vertical temperature profile of the borehole is represented. This includes the pipe temperature $T^{(P)}$,

annulus temperature $T^{(A)}$ and the pipe walls surface temperature $T^{(S)}$. Worth noting that $T^{(S)}$ at the bottom of the well (in the DC section) has a different behaviour than the other of the well. This behaviour resulted from the bigger cross-section area of the DC relative to the DP and the HWDP which lead to different heat transfer coefficients, especially in the annulus section.

On the right of this plot, another three subplots can be seen. The top plot shows the inlet and the outlet fluid temperature with time. At the bottom of the figure, two radial temperature profiles are presented at different depths.

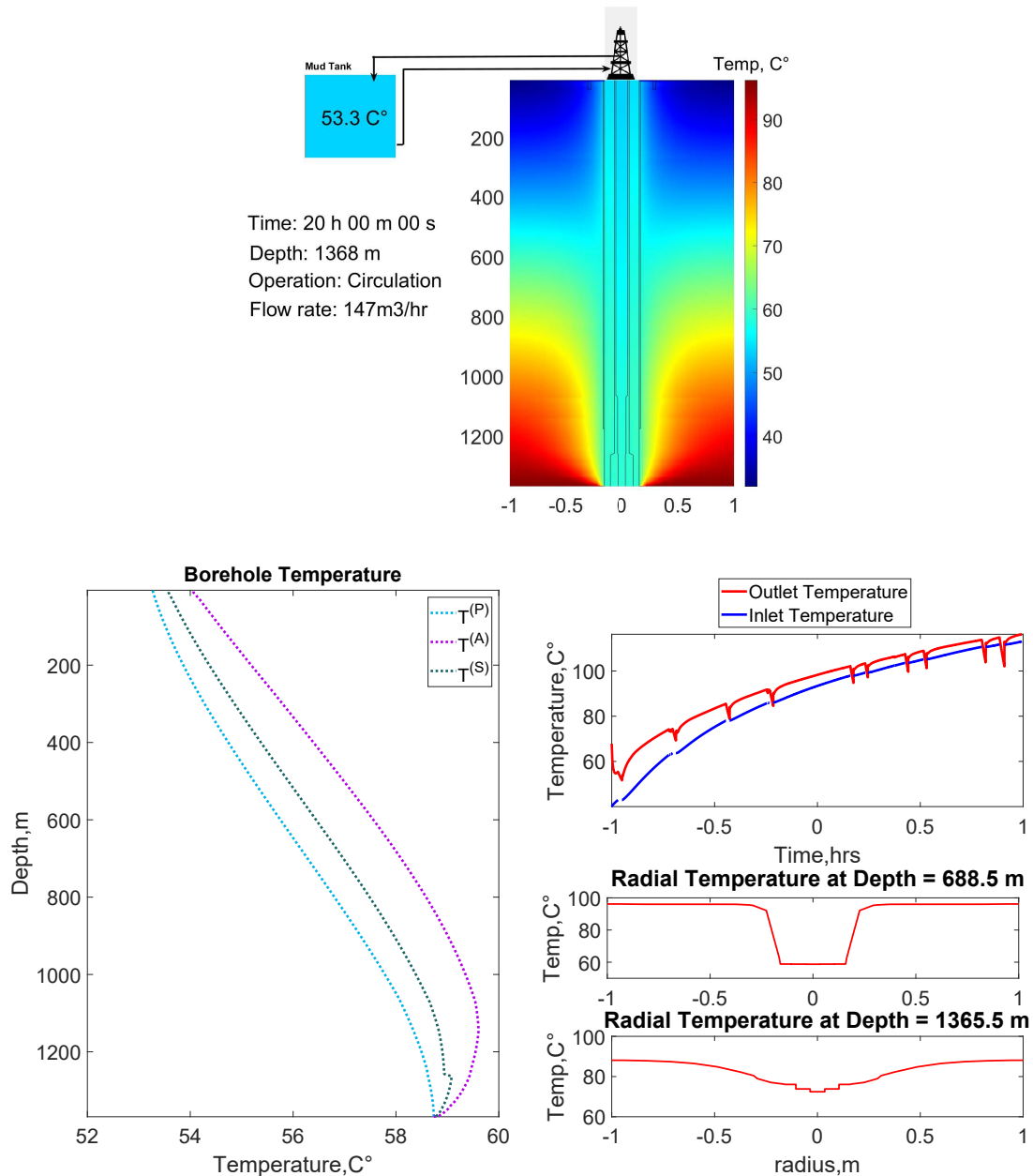


Figure 7. Final result graphical output of the thermal simulation process of GBGT-1 well for the interval between 1251.5 m to 1368 m

A comparison between the measured and the simulated outlet fluid temperature is presented in fig.fig:genesyscomparison.

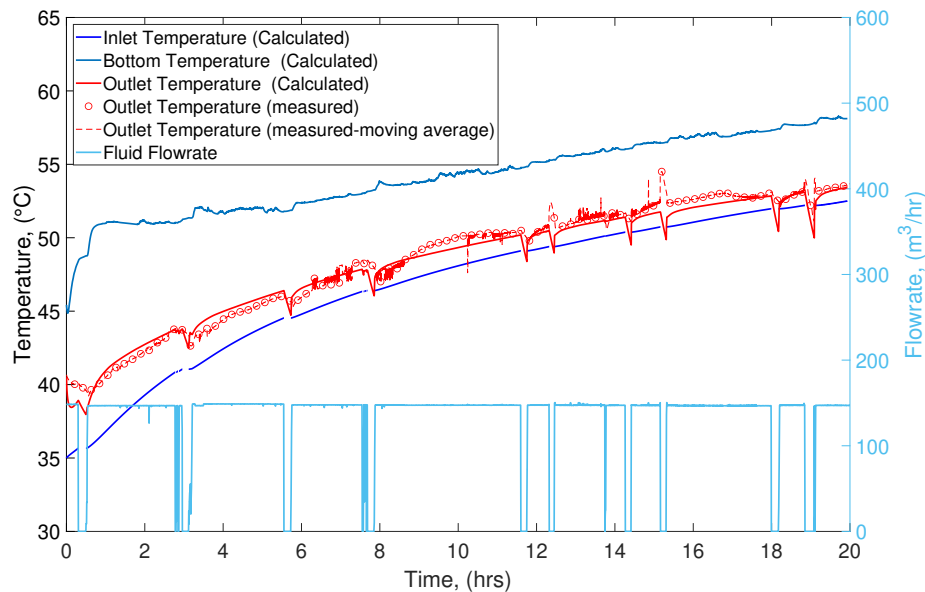


Figure 8. Simulation results for the inlet outlet and bottom hole temperature in comparison with the measured field data from GBGT-1 well

A good match between the simulated and the measured outlet temperature can be seen from the figure. A direct impact on the outlet temperature can be noticed according to the flowing status. The simulated and the measured outlet surface temperature follows the same behaviour during the shut-in condition. As the fluid stop flowing, the surface outlet temperature starts to decrease as it is affected by the surface ambient temperature. A variation in the bottom hole temperature is also noticeable, However, the bottom hole temperature is highly affected by other drilling parameters like the weight on the bit, and the bit rotational speed RPM. To quantify the error, the L^2 relative error norm is $L^2_{error} = 0.0048$ for the outlet temperature using the measured data as the reference.

5 Conclusions

In this work, a demonstration of the coupling between a wellbore temperature model and a comprehensive simulator virtual drilling simulator was presented. The solution algorithm of the thermal model for dynamic real-time temperature simulation has been presented. The model successfully simulated the temperature during drilling the intermediate section of the geothermal well GBGT-1. The results are compared with the field measured data which shows a good agreement with the simulated temperature. Coupling the thermal model with different physical downhole models can lead to better simulation of the drilling process.

Acknowledgements. The authors would like to thank the Federal Institute for Geosciences and Natural Resources (BGR) for providing the drilling data related to the Genesys Groß Buchholz Gt 1 well.

Authorship statement. The authors hereby confirm that they are the sole liable persons responsible for the authorship of this work, and that all material that has been herein included as part of the present paper is either the property (and authorship) of the authors, or has the permission of the owners to be included here.

References

- [1] R. Dirksen. Upgrading formation-evaluation electronics for high-temperature drilling environments. *Journal of Petroleum Technology*, vol. 63, n. 01, pp. 24–26. SPE, 2011.
- [2] K. Fattah, S. El-Katatney, and A. Dahab. Potential implementation of underbalanced drilling technique in egyptian oil fields. *Journal of King Saud University - Engineering Sciences*, vol. 23, n. 1, pp. 49 – 66, 2011.
- [3] J. Zhang, Y. Lu, Y. Chen, and H. Jindong. Effect of temperature recovery on time-dependent wellbore stability in geothermal drilling. ARMA-CUPB-19-4482, 2019.

- [4] E. Cayeux. Time, pressure and temperature dependent rheological properties of drilling fluids and their automatic measurements. SPE, 2020.
- [5] M. R. Annis. High-temperature flow properties of water-base drilling fluids. *Journal of Petroleum Technology*, vol. 19, n. 08, pp. 1074–1080, 1967.
- [6] F. Wang, X. Tan, R. Wang, M. Sun, L. Wang, and J. Liu. High temperature and high pressure rheological properties of high-density water-based drilling fluids for deep wells. *Petroleum Science*, vol. 9, n. 3, pp. 354–362, 2012.
- [7] Z. Vryzas, V. C. Kelessidis, L. Nalbantian, V. Zaspalis, D. I. Gerogiorgis, and Y. Wubulikasimu. Effect of temperature on the rheological properties of neat aqueous wyoming sodium bentonite dispersions. *Applied Clay Science*, vol. 136, pp. 26–36, 2017.
- [8] I. Ohenhen, S. O. Ogiriki, I. Imuetiyan, and O. Ezeja. Experimental study of temperature effect on drilling mud with local additives. *International Journal of Engineering Research in Africa*, vol. 38, pp. 9–16, 2018.
- [9] E. Ataga and J. Ogbonna. Accurate estimation of equivalent circulating density during high pressure high temperature (hpht) drilling operations. SPE-162972-MS, 2012.
- [10] S. K. Choi and C. P. Tan. Modelling of effects of drilling fluid temperature on wellbore stability. SPE-47304-MS, 1998.
- [11] G. Chen and R. T. Ewy. Thermoporoelectric effect on wellbore stability. *SPE Journal*, vol. 10, n. 02, pp. 121–129, 2005.
- [12] H. I. AlBahrani, A. Al-Qahtani, O. Hamid, and Z. Al-Hassan. An investigation of the relationship between the time-dependent wellbore stability and the related operational practices. D032S005R019, 2018.
- [13] Q. Li, Y. Cheng, G. Wang, j. Wei, J. Ding, C. Yan, and Z. Han. Determination of safe mud temperature window for drilling operation in hydrate deposits in shenhu area, northern south china sea. ISOPE-I-19-664, 2019.
- [14] Z. Chen and R. J. Novotny. Accurate prediction wellbore transient temperature profile under multiple temperature gradients: Finite difference approach and case history. SPE-84583-MS, 2003.
- [15] M. M. Abdelhafiz, L. A. Hegele, and J. F. Oppelt. Temperature modeling for wellbore circulation and shut-in with application in vertical geothermal wells. *Journal of Petroleum Science and Engineering*, vol. 204, pp. 108660, 2021.
- [16] M. M. Abdelhafiz, L. A. Hegele, and J. F. Oppelt. Numerical transient and steady state analytical modeling of the wellbore temperature during drilling fluid circulation. *Journal of Petroleum Science and Engineering*, vol. 186, pp. 106775, 2020.
- [17] F. P. Incropera. *Fundamentals of Heat and Mass Transfer*. John Wiley & Sons, Inc., Hoboken, NJ, USA, 2006.
- [18] H. Hu, Z. Guan, B. Wang, B. Lu, W. Chen, Y. Xu, and Y. Liu. Research on weight-on-bit self-adjusting dual-diameter pdc bit design and effect evaluation utilizing stress-releasing effect of rock at bottomhole. *Arabian Journal for Science and Engineering*, vol. 46, n. 7, pp. 6925–6937, 2021.
- [19] D. A. Glowka and C. M. Stone. Thermal response of polycrystalline diamond compact cutters under simulated downhole conditions. *Society of Petroleum Engineers Journal*, vol. 25, n. 02, pp. 143–156, 1985.
- [20] D. Systems. Advanced drilling simulator technology solutions, 2021.
- [21] M. Reddy. Chapter 1 - introduction. In M. Reddy, ed, *API Design for C++*, pp. 1–19. Morgan Kaufmann, Boston, 2011.
- [22] A. Hesshaus, G. Houben, and R. Kringel. Halite clogging in a deep geothermal well – geochemical and isotopic characterisation of salt origin. *Physics and Chemistry of the Earth, Parts A/B/C*, vol. 64, pp. 127–139. Coupled Physical and Chemical Transformations Affecting the Performance of GeoSystems, 2013.